Geomechanics and Engineering, *Vol. 31, No. 3 (2022) 281-289*
https://doi.org/10.12989/gae.2022.31.3.281

Characteristics of soybean urease induced $CaCO_3$ precipitation

Liping Zhu[1,2a], Chaopeng Lang[3b], Bingyan Li[4c], Kejun Wen[5d] and Mingdong Li*[4]

[1]*School of Water Resources and Environmental Engineering, East China University oftechnology, Nanchang, 330013, China*
[2]*Key Laboratory of Ministry of Education for Geomechanics and Embankment Engineering, Hohai University, Nanjing, 210098, China*
[3]*Chongqing Wanzhou District Housing Management Center, Chongqing, 404000,China*
[4]*School of Civil and Architectural Engineering, East China University of Technology, Nanchang 330013, China*
[5]*Department of Civil and Environmental Engineering, Jackson State University, Jackson, MS 39217, USA*

(*Received May 1, 2022, Revised October 12, 2022, Accepted October 28, 2022*)

Abstract. Bio-$CaCO_3$ is a blowout environment-friendly materials for soil improvement and sealing of rock fissures. To evaluate the chemical characteristics, shape, size and productivity of soybean urease induced $CaCO_3$ precipitates (SUICP), experimental studies were conducted via EDS, XRD, FT-IR, TGA, BET, and SEM. Also, the conversion rate of SUICP reaction at different time were determined and analyzed. The Bio-$CaCO_3$ product obtained by SUICP is comprehensively judged as calcite based on the results of EDS, XRD and FT-IR. The SUICP calcite precipitates are detected as spherical or ellipsoidal particles 3-6 μm in diameter with nanoscale pores on their surface, and this morphology is novel. The median secondary particle size d_{50} is 39-88 μm, indicating the agglomeration of the primary calcite particles. The Bio-calcite decomposes at 650-780°C, representing a medium thermal stability. The conversion rate of SUICP reaction can reach 80% in 24h, which is much more efficient than microbially induced $CaCO_3$ precipitation. These results reveal the knowledges of SUICP, and further direct its engineering applications. Moreover, we show an economic channel to obtain porous spherical calcite.

Keywords: $CaCO_3$; calcite; calcium carbonate; EICP; MICP; morphology; urease

1. Introduction

As an effective component for soil improvement and sealing of rock fissures, $CaCO_3$ has been attracting much attentions (Zhao *et al.* 2016, Feoktistova *et al*. 2020, Saulat *et al.* 2020, Feng *et al.* 2021, Kumar *et al.* 2021, Yang *et al.* 2022). It has been successfully used to repair concrete cracks(Qian *et al.* 2021b), to prepare precast concrete piles(Xiao *et al.* 2021), to prevent efflorescence of mortar(Chen *et al.* 2021), to commentate glass beads (Xiao *et al.* 2019), to improve soil (Gao *et al.* 2019, Xu *et al*. 2021) and to preserve cultural relics (Xu *et al*. 2020).

Bio-$CaCO_3$ has a greater adhesion than $CaCO_3$ from chemical technology (Qian *et al.* 2021a), indicating its better effect for soil improvement (Wen *et al.* 2020, Xiao *et al.* 2020, Liu *et al*. 2021). There are several pathways to prepare Bio-$CaCO_3$, including biomineralization (He *et al.* 2019), microbially induced $CaCO_3$ precipitation (MICP) (Zhao *et al.* 2014), enzyme induced $CaCO_3$ precipitation(EICP) (Li *et al.* 2016), biomimetic synthesis (Liu *et al*. 2017), etc. It has been proved that MICP is more productive than chemical pathways (Qian *et al.* 2021a).

EICP, which is presented in Eqs. (1) and (2), is an emerging method to produce Bio-$CaCO_3$ (Carmona *et al.* 2016, Choi *et al.* 2017, Chandra *et al.* 2021, Cui *et al.* 2021). The $CaCO_3$ from EICP can effectively enhance the strength of construction materials by filling pores and bonding particles (Cui *et al.* 2020). Soybeans, jack beans, watermelon seed, pumpkin seed and some other beans can be used as the plant source of urease (Javadi *et al*. 2018). Jack bean urease is fruitful for its high urea hydrolysis activity (Almajed *et al.* 2020a, Almajed *et al*. 2020b), while soybean urease is popular for its availability and economical efficiency (Gao *et al*. 2019, He *et al.* 2020, He *et al.* 2021).

$$NH_2\text{-}CO\text{-}NH_2 + 2H_2O \xrightarrow{\text{soybean urease}} CO_3^{2-} + 2NH_4^+ \quad (1)$$

$$Ca^{2+} + CO_3^{2-} \rightarrow CaCO_3 \quad (2)$$

We noticed that the bio-$CaCO_3$ prepared by soybean urease induced $CaCO_3$ precipitation (SUICP) was different from that prepared by MICP in shape (Zhao *et al*. 2014, Wu *et al*. 2020). Thus, a series of experimental studies were arranged and conducted, aiming to discover the chemical characteristics, shape, size and productivity of SUICP. The results are presented in this paper, which will raise the awareness of SUICP and direct its engineering applications.

*Corresponding author, Professor
E-mail: lmd@ecut.edu.cn
[a]Ph.D. student
E-mail: m20l@163.com
[b]Master
E-mail: 15870696133@163.com
[c]Master
E-mail: ysrolan@ecut.edu.cn
[d]Ph.D.
E-mail: kejun.wen@jsums.edu
[e]Professor
E-mail: lmd@ecut.edu.cn

ISSN: 2005-307X (Print), 2092-6219 (Online)

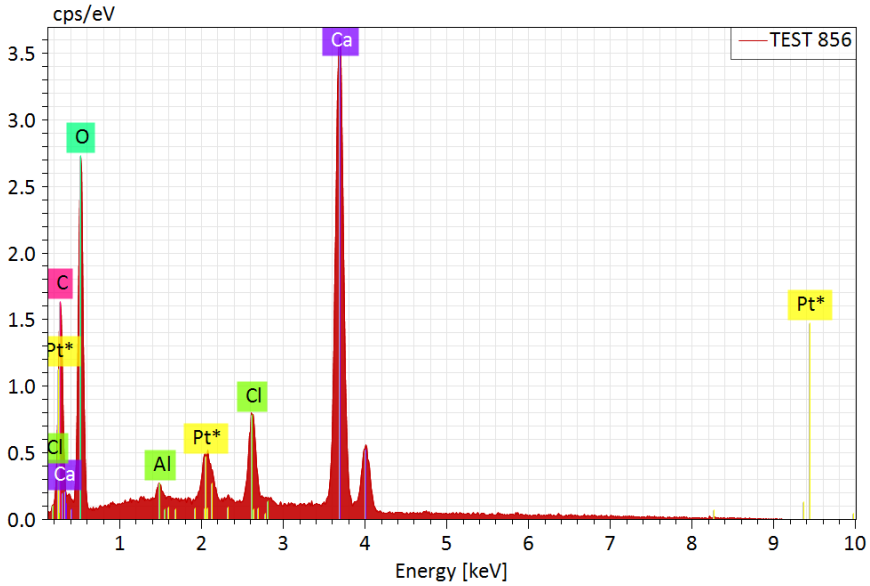

Fig. 1 The EDS spectrum of SUICP

Table 1Components of the cementation solutions

Marker	Deminized water (mL)	$CaCl_2$ (g)	Urea (g)	Concentration (M)
C1	1000	222	120	1
C2	1000	444	240	2

2. Materials and methods

2.1 Preparation of soybean urease solutions (SUS)

Ureases are a class of urea-hydrolyzing enzymes which can be extracted from bacteria or plants (Wu *et al.* 2019). The urease utilized in this work was extracted from soybeans. Dry soybeans were crushed with a grinder and sent through a 100-meshsieve. 100 g soybean power was put into 1000 mL deminized water and stirred for 6 h at 4°C.SUS was the supernatant obtained by centrifuging the previous solution at 3000 r $min^{-1}$for 15 min.

2.2Cementationsolution (CS)

The CS for SUICP were mixed solutions of analytical grade urea(CH_4N_2O purity≥99%) and anhydrous calcium chloride($CaCl_2$)at two concentrations(1 M, 2 M) according to Table 1.

2.3 Preparation of SUICP specimens

Equal amounts of SUS and CS were mixed and stirrer in a beaker. The beaker was put in a refrigerator to keep a 4°C environment, and SUICP was ongoing. After 24h, the precipitates were filtered and then abstersived to remove dissolved$CaCl_2$ and urea. They were then oven-dried at 101°C for 24h (Pan *et al.* 2020) to obtain SUICP specimens. The specimen made from cementation media C1 was marked as P1, and similarly the other specimen made from cementation media C2 was marked as P2.

2.4 Characterization of SUICP

EDS tests were conducted to determine the chemical compositions of the SUICP samples with qualitative and quantitative analysis of the obtained characteristic spectral lines. To determine the mineral composition of SUICP, high-resolution XRD tests were performed on a dandong DX-2700 diffractometer with a scan step of 2θ 0.02°and a scan speed of 10° min^{-1} in the 2θ range from 10° to 90°. Working voltage and current were 40 kV and 250 mA, respectively. The infrared spectrum was recorded on a 470FT-IR instrument using KBr pellets. The thermal stability of SUICP was studied via TGA under air condition in the temperature range from 100°C to 1000°C at a heating rate of 20°Cmin^{-1}. To investigate the crystal shape, surface morphologies were characterized with field-emission SEM(TM-1000) at 20.00 kV. The magnification was 1,000×–30,000×. Specific surface area was analyzed by Brunauer-Emmett-Tellert(BET) technique with N_2 as an absorbed gas. Particle size distributions were analyzed by a laser scattering particle size analyzer with water as dispersing agent at a pump speed of 2680r/min.

3. Results and discussions

3.1 Chemical characteristics of SUICP

The EDS spectrum of SUICP is shown in Fig. 1. The featured peaks are correspondent to the following elements: Ca, C, O, Cl, and Pt. Cl element is from the ammonium chloride byproduct in Eq. (2), while Pt is the sputter coating for sample preparation. Further, the quantitative results are listed in Table 2. The main elements Ca, O and C account for the highest amounts, which are 48.18%, 35.82%, and 10.56%, respectively. The correspongding Carbon-to-Oxygen ratio is about 1 to 3, and the Calcium-to-Carbon ratio is about 1 to 1, which are the appropriate ratios for

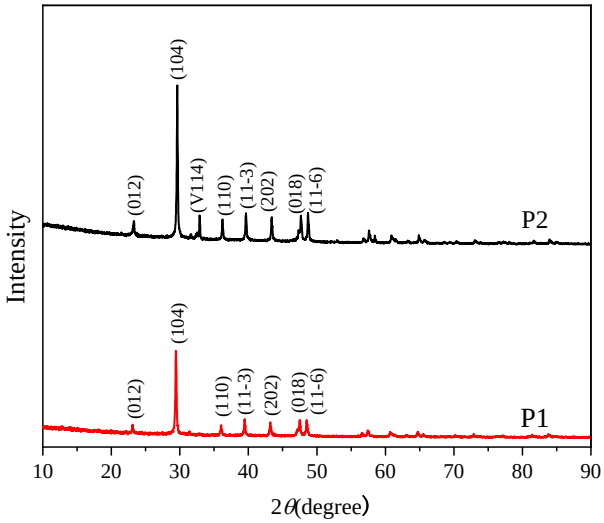

Fig. 2 XRD patterns of SUICP specimens

Table 2 The quantitative compositions of SUICP

Elements	Mass (%)	Number (%)	Abs. Error (%)
O	35.82	49.98	3.37
Ca	48.18	26.84	1.20
C	10.56	19.63	1.11
Cl	4.80	3.02	0.15
Al	0.63	0.52	0.05
Pt	0.00	0.00	0.00
Sum	100.00	100.00	/

calcium carbonate. Thus, the precipitates maybe calcium carbonate based on the EDS results (Zhao *et al.* 2019).

The applications of $CaCO_3$ are closely related to phase composition and particle shape. There are three polymorphs of $CaCO_3$ to exist, which are calcite, aragonite and vaterite (Zhuravlev and Atuchin 2020). Calcite is commonly rhomboid cube-shaped. It is widespread used in cement and other construction materials for its best thermodynamically stablility and superior mechanical strength (Liu *et al*. 2017). Aragonite is usually needle-shaped and it is thermostable (Kanoje *et al.* 2018). Vaterite has spherical particles and shows great potential for biomedical applications. Fig. 2 demonstrates the XRD patterns of SUICP crystals. Their diffraction angles are 23.1°, 29.4°, 35.9°, 39.5°, 43.1°, 47.3°, and 48.5°, exactly corresponding to the characteristic peaks of calcite (012) (104), (110), (11-3), (202), (018), and (116), respectively. There are no characteristic peaks of other calcium carbonate crystal forms (vaterite or aragonite, PDF: 47–1743). Therefore, the main component of SUICP is calcite, which is the same as that of MICP (Zhao *et al.* 2014). The most intense peak in the SUICP is related to C(104), which is similar to EICP obtained from ACROS organics (Wen *et al.* 2020). By contrast, the diffraction peaks of P2 are stronger than that of P1, indicating that superior solution concentration of CS favors SUICP reaction.

Crystal types of SUICP can be distinguished by internal vibration mode of CO32− radical(v1,symmetric stretching vibration, 1530–1320 cm−1; v2, out-of-plane bending vibration, 1100–1040 cm−1; v3, asymmetric stretching vibration, 890–800 cm−1, and v4, in-plane bending vibration, 745–670 cm−1) (Ren *et al*. 2015). The vibration modes v2 and v4 are used to distinguish $CaCO_3$ crystal with the assistance of FT-IR spectrum. As seen in Fig. 3, v2 peaks and v4 peaks of the both specimens P1 and P2 occur at 837-712 cm−1, being correspondent to the characteristic absorption peaks of calcite (Islam *et al*. 2013). The absorption band at 2513 cm−1 indicates the existence of carbonate asymmetrical vibration. The absorption bands at 866 cm−1 and 1074 cm−1 indicates that there is no hydrated phase existed (Dyer *et al*. 2016). Additionally, the peak at 711 cm−1 is corresponding to v4 of O-CO- in calcite (Wang *et al.* 2018). In conclusion, the crystal type of SUICP is verified as calcite, which is consistent with the judgment by XRD results.

There are three phases in the thermogravimetric (TG) curve of Bio-$CaCO_3$ obtained from SUICP (Fig. 4). In Phase 1, an initial weight loss of 17% occurs between 100°C and 656°C, which is associated with the dissipation of hygroscopic water. The second phase is corresponding to the second weight loss, which is much sharper than phase 1. It occurs in the temperature range of 656°C–780°C with a weight loss of 32.63%, which is due to the decomposition of calcite crystal (Lee *et al.* 2016), as presented in Eq. (3). There should be a weight loss of 44% based on Eq. (3), and the experimental weight loss in this stage reaches 40%, indicating as much as 90% Bio-$CaCO_3$ decomposed in this stage. When the temperature is higher than 780°C, there is no more chemical change, and the TG curve accordingly turns into stable phase. Bushuev et al.(2015) reported that $CaCO_3$ decomposed in the temperature range of 300°C–850°C. The decomposition of Bio-$CaCO_3$ from SUICP began at 656°C, being consistent with his findings. Morandeau *et al*. (2014) reported that well-crystallized calcite decomposed in the range of 750°C–900°C. The TGA results indicate that Bio-$CaCO_3$ obtained from SUICP is medium-crystallized calcite with a correspondent moderate thermal stability.

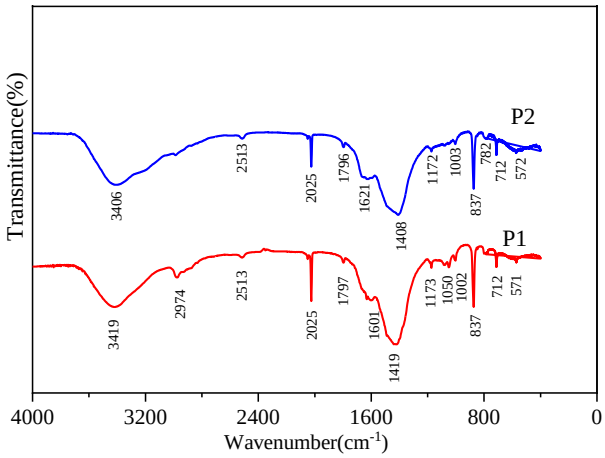

Fig. 3 FT-IR spectrums of SUICP specimens

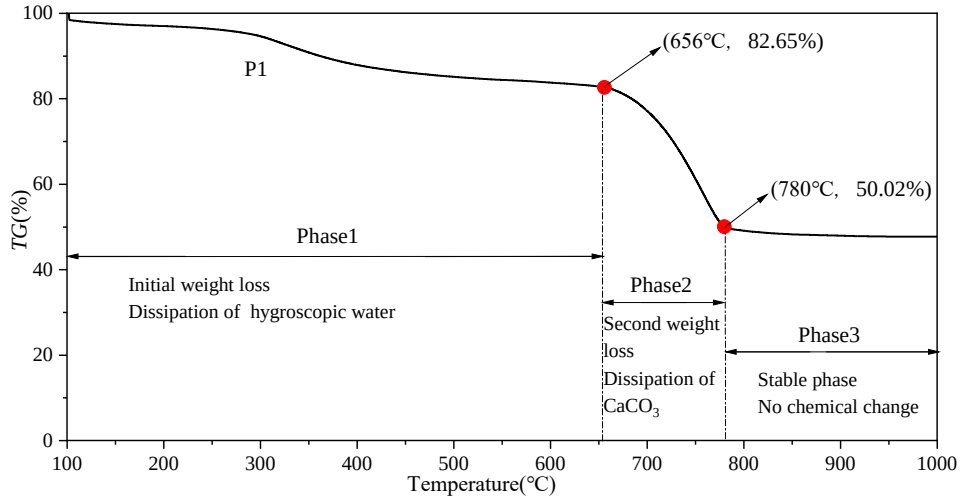

Fig. 4 TG curve of SUICP

$$\text{SUICP calcites} \qquad CaO+CO_2\uparrow \qquad (3)$$

3.2 Shape and size of SUICP calcite

The microscopic morphologies of SUICP detected via SEM are showed in Fig. 5. The calcite crystals are spherical or ellipsoidal with a diameter of 3-6 μm (Fig. 5(c)). It also reveals that the calcite exists primarily as aggregates (Fig. 5(a) and 5(b)). By comparison, those calcite particles induced by urease from watermelon seed were observed as rhombic with a particle size of 2-4 um (Javadi *et al*. 2018), as showed in Fig. 6(a). The calcites induced by *Sporosarcina pasteurii*bacteria were observed as rhombic with a particle size of 10-80 um (Zhao *et al.* 2014, Li *et al*. 2016), as showed in Figs. 6(b) and 6(c). The calcites induced by urease from jack beans (Canavalia ensiformis) was observed as cuboid (Nam *et al.* 2015), as showed in Fig. 6(d).

Spherical calcium carbonate has unique advantages in several industries due to its outstanding characteristics of good fluidity, dispersity, smoothness, large specific surface area, and small density (Kim *et al.* 2010, Tao *et al*. 2015, Aliotta *et al.* 2019). Spherical calcium carbonate can be prepared through carbonization reaction involving various amino acids as organic additives (Lai *et al*. 2015). Moreover, multiple organic additives (e.g., fatty acids, octadecyl dihydrogen phosphate) with specific functional groups were successfully used as crystal morphology regulators of $CaCO_3$ (Hait *et al*. 2013, Chen *et al*. 2018, Yang *et al.* 2022). So a possible reason for the spherical or ellipsoidal shape of the produced calcite in current study is the existence of other soluble proteins in soybeans except for urease, especially the presence of carboxyl (-COO-) and -NH-CO- groups in the protein molecules. Ca^{2+} ions become enriched on these groups, and then attract CO_3^{2-} ions, which causes the oversaturation of local $CaCO_3$ near the organic matrix, leading to the heterogeneous nucleation of $CaCO_3$ (Chen *et al*. 2010).

The latest reports indicated a trend of preparing nanoscale spherical $CaCO_3$ for promising intracellular delivery application (Trushina *et al.* 2016, Palmqvist *et al.* 2017, Wang *et al*. 2019, Feoktistova *et al*. 2020). The most common pathways include biomineralization biomimetic synthesis, carbonation, double decomposition, and microemulsion (Lei *et al*. 2015, Elsharkawy *et al.* 2018).

From Fig. 2(d), the morphology at 30,000×, lots of nano-size pores can be recognized on the surface of the

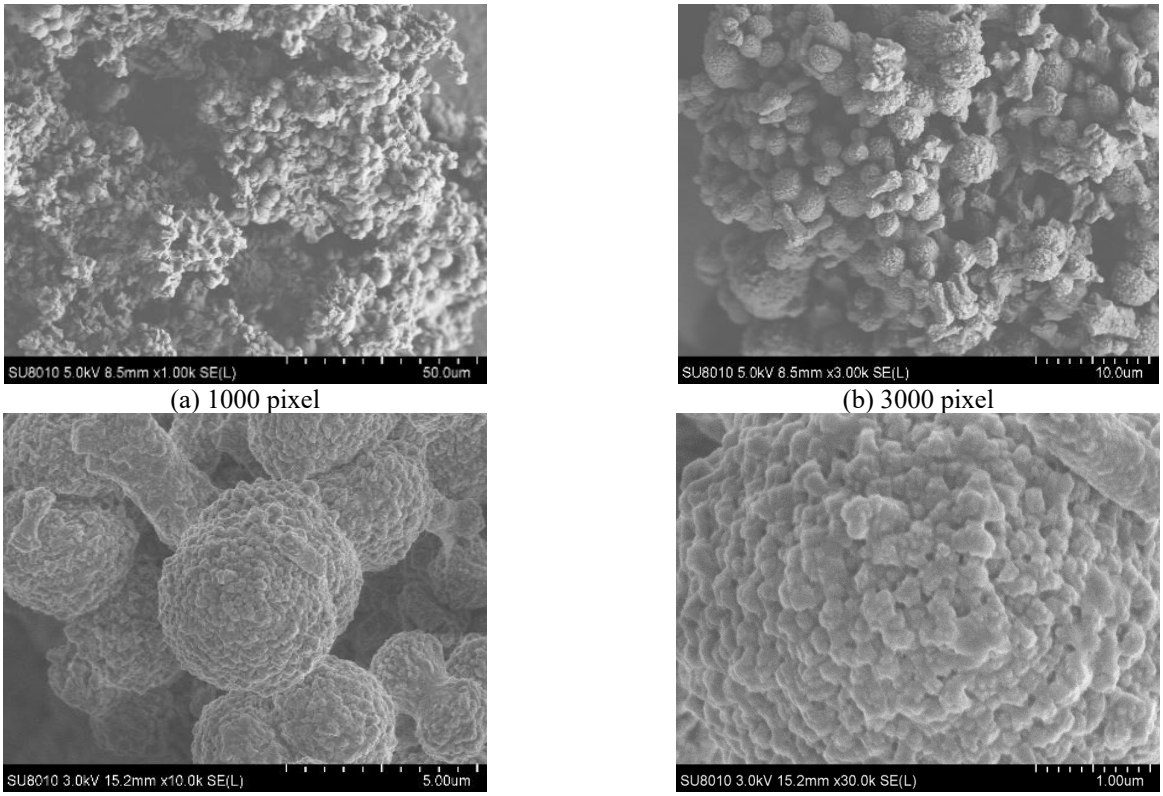

(a) 1000 pixel (b) 3000 pixel

(c) 10000 pixel (d) 30000 pixel

Fig. 5 SEM morphologies of SUICP under four different pixels

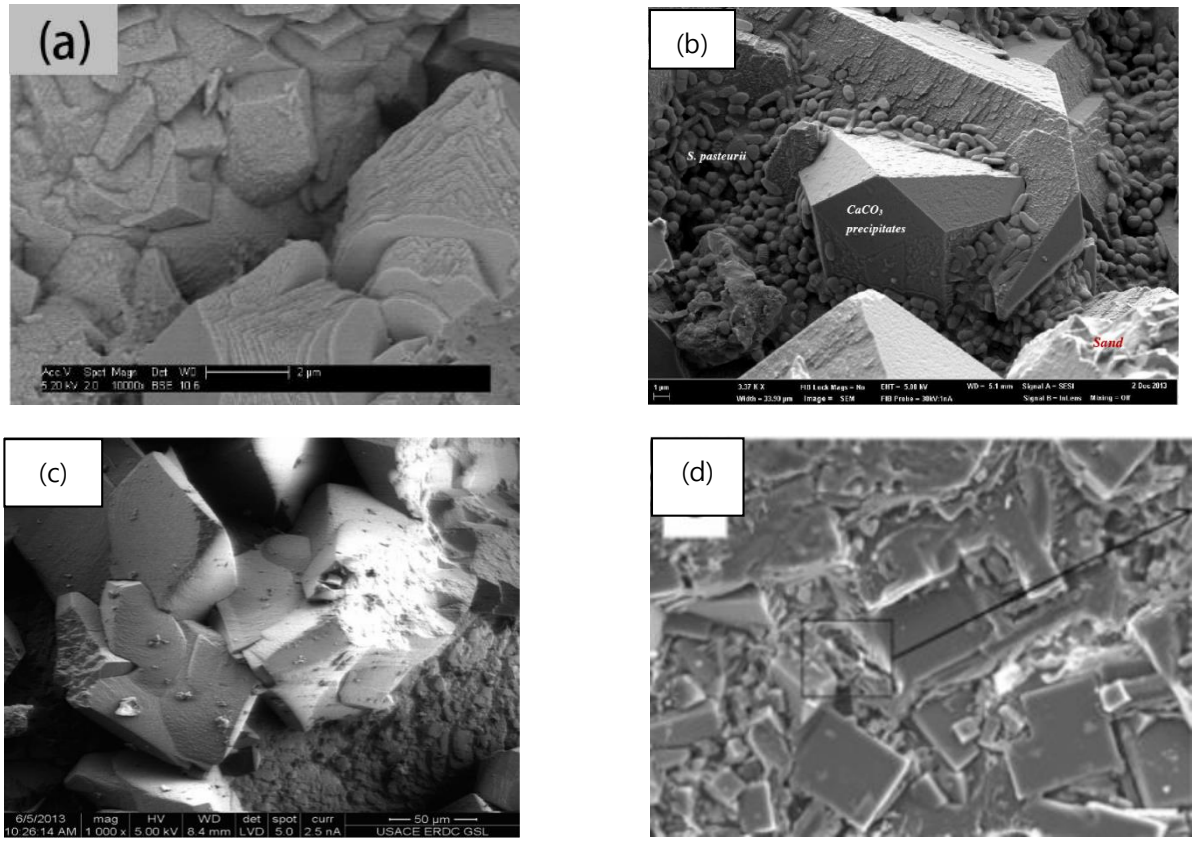

Fig. 6 SEM morphologies of related calcite crystals (a) Javadi *et al.* (2019), (b) Li *et al*. (2016), (c) Zhao *et al.* (2014) and (d) Nam *et al.* (2015)

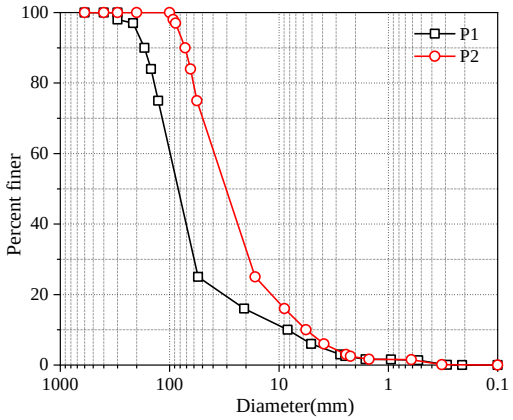

Fig. 7 Particle size distribution curves of SUICP

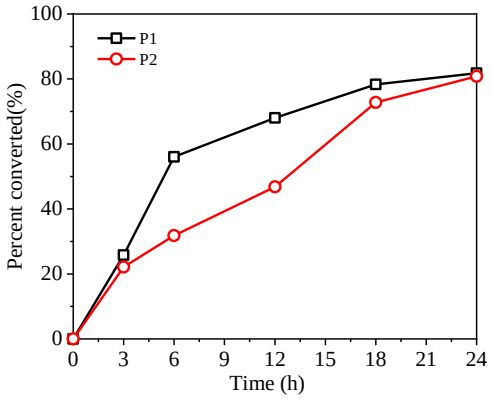

Fig. 8 Generation rate of SUICP

SUICP calcite. Similar porous $CaCO_3$ microsphere exhibited good delivery properties for doxorubicinare (Li *et al.* 2020). As a result, the calcite with nano-scale pores, as prepared in this work has the potential function of pollutant treatment and drug delivery.

The specific surface areas of SUICP specimens P1 and P2 were determined as 138.5 $m^2kg^{-1}$and 185.6 m^2kg^{-1}, respectively. Based on the report by Yang and Shih (2010), the primary particle size of SUICP can be calculated by Eq. (4), which are 16 μm and 12 μm, respectively.

$$d=6/(s_g\rho_g) \tag{4}$$

where s_g is the specific surface area, and ρ_g is the gravity of calcium carbonate, which can be assumed as equal to 2.71 g/cm^3.

Fig. 7 shows the particle size distribution (secondary particle size distribution) curves of P1 and P2. The median secondary particle size d_{50} of P1 and P2 are 88.49 and 38.77 μm, respectively. It can be seen that the secondary particles of SUICP are much coarser than the primary particles, which indicates the agglomeration of the primary particles because of their large specific surface area (Bang *et al.* 2012). As for the smaller median secondary particle size of P2 than that of P1, the possible reason is that the superior dissolved $CaCl_2$ in CS reduced the adsorption forces among the primary calcite particles.

3.3 Rate of generation

After the mixing of SUS and CS, the precipitates were collected at different time, equal to 3, 6, 12, 18, and 24h, respectively. The mass of the collected precipitates was determined as m_c, and the correspondent generation rates of calcite were calculated by Eq. (5).

$$gr_c=\frac{\frac{m_c}{mw_c}}{v_{cm}\times c_{cm}}\times 100\% \tag{5}$$

where: mw_c is the molecular weight of calcite, which can be assumed as 100 g mol^{-1}.
v_{cm} is the volume of CS.
c_{cm} is the concentration of CS.

As shown in Fig. 8, the calcite generation rates increase with time within 24h, reaching 81.8% and 80.8% for P1 and P2, respectively. The results manifest high calcite generation efficiency of SUICP and high urea hydrolysis capacity of SUS. Being compared with the results by Wen *et al.* (2020) and Li *et al.* (2018) , SUICP provide a higher calcite generation efficiency than MICP or EICP by ACROS organics enzyme

3.4 Summaries on comparison of Bio-$CaCO_3$s induced by different Urease source

As a summary, the characteristics of Bio-$CaCO_3$ obtained from SUICP are compared with results of references, as listed in Table 3.

Table 3 Comparison of the obtained Bio-$CaCO_3$ with results of references

Bio-$CaCO_3$	Conversion rate (%)	Crystal types	Crystal morphology	Urease source
SUICP (This work)	81.8%, 80.8%	calcite	Spherical	Soybean
EICP (Cui *et al*. 2021)	42%	calcite	Rhombic	Urease extracted from bacteria *Sporosarcina pasteurii*
EICP (Nam *et al*. 2015)	27%	calcite and vaterite	Rhombicand rhombic	Canavalia ensiformis
EICP (Song *et al*. 2020)	75%	vateriteand calcite	Sphericaland rhombic	Soybean
EICP (Park *et al*. 2022)	64%	calcite	Rhombic	Soybean
EICP (Yuan *et al*. 2020)	71.44%	calcite	striped and rhombic	Sigma Aldrich
MICP (Cui *et al*. 2021)	81%	calcite	Rhombic and Spherical	*Sporosarcina pasteurii*

4. Conclusions

Based on the results of EDS, XRD and FT-IR, the Bio-$CaCO_3$ from SUICP is comprehensively judged as calcite. The SUICP calcite crystal shapes are detected as spherical or ellipsoidal of 3-6 μm in diameter with nanoscale pores on its surface, which are novel. The median secondary particle size d_{50} of SUICP specimens P1 and P2 are 88 and 39 μm, respectively, which are much coarser than the primary particle size, indicating the agglomeration of the primary particles. The SUICP calcites decompose at the temperature of 650-780°C, representing a calcite from of medium thermal stability. The generation rate of SUICP can reach 80% in 24h, demonstrating an extremely high productivity. This study provides the knowledge of SUICP, and further directs its engineering applications. Moreover, we show an economical channel to obtain porous spherical calcite.

Acknowledgements

This research is based upon work supported by the National Foundation of China under Grant No. 51869001 and No. 52168043, Key Research and Development Program of Jiangxi Province under Grant No. 20202BBG73037, Open Fund from Engineering Research Center for Geological Environment and Underground Space of Jiangxi Province (JXDHJJ2021-013) as well as Shuangqian Innovative Talents of Jiangxi(Mingdong Li) and Young Jinggang Scholar(Mingdong Li).

Competing interests

The authors declare no competing interests.

References

Aliotta, L., Cinelli, P., Coltelli, M.B. and Lazzeri, A. (2019), "Rigid filler toughening in PLA-Calcium Carbonate composites: Effect of particle surface treatment and matrix plasticization", *Eur. Polymer J.*, **113**, 78-88. http://doi.org/10.1016/j.eurpolymj.2018.12.042.

Almajed, A., Abbas, H., Arab, M., Alsabhan, A., Hamid, W. and Al-Salloum, Y. (2020), "Enzyme-Induced Carbonate Precipitation (EICP)-Based methods for ecofriendly stabilization of different types of natural sands", *J. Cleaner Production*, **274**, 122627. https://doi.org/10.1016/j.jclepro.2020.122627.

Almajed, A., Lemboye, K., Arab, M.G. and Alnuaim, A. (2020), "Mitigating wind erosion of sand using biopolymer-assisted EICP technique", *Soils Found.*, **60**(2), 356-371. https://doi.org/10.1016/j.sandf.2020.02.011.

Bang, J.H., Jang, Y.N., Kim, W., Song, K.S., Jeon, C.W., Chae, S. C. and Lee, M.G. (2012), "Specific surface area and particle size of calcium carbonate precipitated by carbon dioxide microbubbles", *Chem. Eng. J.*, **198**, 254-260. https://doi.org/10.1016/j.cej.2012.05.081.

Bushuev, Y.G., Finney, A.R. and Rodger, P.M. (2015), "Stability and structure of hydrated amorphous calcium carbonate", *Crystal Growth Design*, **15**(11), 5269-5279. https://doi.org/10.1021/acs.cgd.5b00771.

Carmona, J.P., Oliveira, P.J.V. and Lemos, L.J. (2016), "Biostabilization of a sandy soil using enzymatic calcium carbonate precipitation", *Procedia Eng.*, **143**, 1301-1308. https://doi.org/10.1016/j.proeng.2016.06.144.

Chandra, A. and Ravi, K. (2021), "Application of enzyme-induced carbonate precipitation (EICP) to improve the shear strength of different type of soils", In *Problematic soils and geoenvironmental concerns* (pp. 617-632). Springer, Singapore. https://doi.org/10.1007/978-981-15-6237-2_52.

Chen, L., Shen, Y.H., Xie, A.J. and Cheng, Q.N. (2010), "Biological synthesis of calcite crystals using Scindapsus aureum petioles", *J. Mater. Sci.*, **45**(11), 2938-2943. https://doi.org/10.1007/s10853-010-4286-x.

Chen, T., Shi, P., Li, Y., Duan, T., Yu, Y., Li, X. and Zhu, W. (2018), "Biomineralization of varied calcium carbonate crystals by the synergistic effect of silk fibroin/magnesium ions in a microbial system", *Cryst. Eng. Comm.*, **20**(17), 2366-2373. https://doi.org/10.1039/c8ce00099a.

Chen, Y. and Qian, C. (2021), "A new method for anti-efflorescence of mortar by bio-mineralization", *Constr. Build. Mater.*, **290**, 123261. https://doi.org/10.1016/J.CONBUILDMAT.2021.123261.

Choi, S.G., Chu, J., Brown, R.C., Wang, K. and Wen, Z. (2017), "Sustainable biocement production via microbially induced calcium carbonate precipitation: Use of limestone and acetic acid derived from pyrolysis of lignocellulosic biomass", *ACS Sustain. Chem. Eng.*, **5**(6), 5183-5190. https://doi.org/10.1021/acssuschemeng.7b02137.

Cui, M.J., Lai, H.J., Hoang, T. and Chu, J. (2021), "One-phase-

low-pH enzyme induced carbonate precipitation (EICP) method for soil improvement", *Acta Geotechnica*, **16**(2), 481-489. https://doi.org/10.1007/s11440-020-01043-2.

Cui, M.J., Zheng, J.J., Chu, J., Wu, C.C. and Lai, H.J. (2021), "Bio-mediated calcium carbonate precipitation and its effect on the shear behaviour of calcareous sand", *Acta Geotechnica*, **16**(5), 1377-1389. https://doi.org/10.1007/s11440-020-01099-0.

Deepika, S., Hait, S. K., Christopher, J., Chen, Y., Hodgson, P. and Tuli, D.K. (2013), "Preparation and evaluation of hydrophobically modified core shell calcium carbonate structure by different capping agents", *Powder Technol.*, **235**, 581-589. https://doi.org/10.1016/j.powtec.2012.11.015.

Denisenko, Y.G., Atuchin, V.V., Molokeev, M.S., Sedykh, A.E., Khritokhin, N.A., Aleksandrovsky, A.S. and Müller-Buschbaum, K. (2022), "Exploration of the crystal structure and thermal and spectroscopic properties of monoclinic praseodymium sulfate $Pr_2 (SO_4)_3$", *Molecules*, **27**(13), 3966. https://doi.org/10.3390/molecules27133966.

Dyer, M. and Viganotti, M. (2016), "Oligotrophic and eutrophic MICP treatment for silica and carbonate sands", *Bioinspired, Biomimetic Nanobiomater.*, **6**(3), 168-183. https://doi.org/10.1680/jbibn.16.00002

Elsharkawy, S. and Mata, A. (2018), "Hierarchical biomineralization: from nature's designs to synthetic materials for regenerative medicine and dentistry", *Adv. Health. Mater.*, **7**(18), 1800178. https://doi.org/10.1002/adhm.201800178

Feng, J., Yang, F. and Qian, S. (2021), "Improving the bond between polypropylene fiber and cement matrix by nano calcium carbonate modification", *Constr. Build. Mater.*, **269**, 121249. https://doi.org/10.1016/j.conbuildmat.2020.121249.

Feoktistova, N.A., Vikulina, A.S., Balabushevich, N.G., Skirtach, A.G. and Volodkin, D. (2020), "Bioactivity of catalase loaded into vaterite $CaCO_3$ crystals via adsorption and co-synthesis", *Mater. Design*, **185**, 108223. https://doi.org/10.1016/j.matdes.2019.108223.

Zou, Z., Habraken, W.J., Matveeva, G., Jensen, A.C., Bertinetti, L., Hood, M.A. and Fratzl, P. (2019), "A hydrated crystalline calcium carbonate phase: Calcium carbonate hemihydrate", *Science*, **363**(6425), 396-400. https://doi.org/10.1126/science.aav0210.

Gao, Y., He, J., Tang, X. and Chu, J. (2019), "Calcium carbonate precipitation catalyzed by soybean urease as an improvement method for fine-grained soil", *Soils Found.*, **59**(5), 1631-1637. https://doi.org/10.1016/j.sandf.2019.03.014.

He, J., Gao, Y., Gu, Z., Chu, J. and Wang, L. (2020), "Characterization of crude bacterial urease for $CaCO_3$ precipitation and cementation of silty sand", *J. Mater. Civil Eng.*, **32**(5), 04020071. https://doi.org/10.1061/(ASCE)MT.1943-5533.0003100.

He, J., Fang, C., Hang, L., Qi, Y., Mao, X., Yan, B. and Gao, Y. (2021), "Enzyme induced carbonate precipitation for soil internal erosion control under water seepage", *Geomech. Eng.*, **26**(3), 289-299. https://doi.org/10.12989/gae.2021.26.3.289.

Islam, K.N., Bakar, M.Z.B.A., Ali, M.E., Hussein, M.Z.B., Noordin, M.M., Loqman, M.Y. and Hashim, U. (2013), "A novel method for the synthesis of calcium carbonate (aragonite) nanoparticles from cockle shells", *Powder Technol.*, **235**, 70-75. https://doi.org/10.1016/j.powtec.2012.09.041.

Javadi, N., Khodadadi, H., Hamdan, N. and Kavazanjian Jr, E. (2018), "EICP treatment of soil by using urease enzyme extracted from watermelon seeds", In *IFCEE 2018*, 115-124. https://doi.org/10.1061/9780784481592.012.

Kim, S. and Park, C.B. (2010), "Dopamine-induced mineralization of calcium carbonate vaterite microspheres", *Langmuir*, **26**(18), 14730-14736. https://doi.org/10.1021/la1027509.

Kumar, D. and Ranade, R. (2021), "Development of strain-hardening cementitious composites utilizing slag and calcium carbonate powder", *Constr. Build. Mater.*, **273**, 122028. https://doi.org/10.1016/J.CONBUILDMAT.2020.122028.

Lai, Y., Chen, L., Bao, W., Ren, Y., Gao, Y., Yin, Y. and Zhao, Y. (2015), "Glycine-mediated, selective preparation of monodisperse spherical vaterite calcium carbonate in various reaction systems", *Crystal Growth Design*, **15**(3), 1194-1200. https://doi.org/10.1021/cg5015847.

Lee, S.W., Kim, Y.J., Lee, Y.H., Guim, H. and Han, S.M. (2016), "Behavior and characteristics of amorphous calcium carbonate and calcite using $CaCO_3$ film synthesis", *Mater. Design*, **112**, 367-373. https://doi.org/10.1016/j.matdes.2016.09.099.

Lei, Y. (2015), "Experimental synthesis and geological significance of calcium carbonate under control of different additives", *Northwest University*.

Li, L., Yang, Y., Lv, Y., Yin, P. and Lei, T. (2020), "Porous calcite $CaCO_3$ microspheres: Preparation, characterization and release behavior as doxorubicin carrier", *Colloids Surfaces B: Biointerfaces*, **186**, 110720. https://doi.org/10.1016/j.colsurfb.2019.110720.

Li, M., Li, L., Ogbonnaya, U., Wen, K., Tian, A. and Amini, F. (2016), "Influence of fiber addition on mechanical properties of MICP-treated sand", *J. Mater. Civil Eng.*, **28**(4), 04015166. https://doi.org/10.1061/9780784480472.002.

Li, M., Wen, K., Li, Y. and Zhu, L. (2018), "Impact of oxygen availability on microbially induced calcite precipitation (MICP) treatment", *Geomicrobio. J.*, **35**(1), 15-22. https://doi.org/10.1080/01490451.2017.1303553.

Liu, S., Du, K., Huang, W., Wen, K., Amini, F. and Li, L. (2021), "Improvement of erosion-resistance of bio-bricks through fiber and multiple MICP treatments", *Constr. Build. Mater.*, **271**, 121573. https://doi.org/10.1016/J.CONBUILDMAT.2020.121573.

Liu, Y., Chen, Y., Huang, X. and Wu, G. (2017), "Biomimetic synthesis of calcium carbonate with different morphologies and polymorphs in the presence of bovine serum albumin and soluble starch", *Mater. Sci. Eng.*, **79**, 457-464. https://doi.org/10.1016/j.msec.2017.05.085.

Morandeau, A., Thiery, M. and Dangla, P. (2014), "Investigation of the carbonation mechanism of CH and CSH in terms of kinetics, microstructure changes and moisture properties", *Cement Concrete Res.*, **56**, 153-170. https://doi.org/10.1016/j.cemconres.2013.11.015.

Nam, I.H., Chon, C.M., Jung, K.Y., Choi, S.G., Choi, H. and Park, S.S. (2015), "Calcite precipitation by ureolytic plant (Canavalia ensiformis) extracts as effective biomaterials", *KSCE J. Civil Eng.*, **19**(6), 1620-1625. https://doi.org/10.1007/s12205-014-0558-3.

Palmqvist, N.M., Nedelec, J.M., Seisenbaeva, G.A. and Kessler, V. G. (2017), "Controlling nucleation and growth of nano-$CaCO_3$ via CO2 sequestration by a calcium alkoxide solution to produce nanocomposites for drug delivery applications", *Acta Biomaterialia*, **57**, 426-434. https://doi.org/10.1016/j.actbio.2017.05.006.

Pan, X., Chu, J., Yang, Y. and Cheng, L. (2020), "A new biogrouting method for fine to coarse sand", *Acta Geotechnica*, **15**(1), 1-16. https://doi.org/10.1007/s11440-019-00872-0.

Park, J. and Choi, B.Y. (2022), "Feasibility study of enzyme-induced calcium carbonate precipitation (EICP) for CO2 leakage prevention", *Geosci. J.*, **26**(2), 279-288. https://doi.org/10.1007/S12303-021-0033-3.

Qian, C., Ren, X., Rui, Y. and Wang, K. (2021a), "Characteristics of bio-$CaCO_3$ from microbial bio-mineralization with different bacteria species", *Biochem. Eng. J.*, **176**, 108180. https://doi.org/10.1016/J.BEJ.2021.108180.

Qian, C., Zheng, T., Zhang, X. and Su, Y. (2021b). "Application of microbial self-healing concrete: Case study", *Constr. Build. Mater.*, **290**, 123226. https://doi.org/10.1016/J.CONBUILDMAT.2021.123226.

Ren, L., Zhang, Q., Zhu, W., Li, Q. and Mao, X. (2015), "Biomimetic synthesis of $CaCO_3$ microrings", *J. Synthetic Crystals*, **44**(1), 250-255. https://doi.org/10.16553/j.cnki.issn1000-985x.2015.01.049.

Saulat, H., Cao, M., Khan, M.M., Khan, M., Khan, M.M. and Rehman, A. (2020), "Preparation and applications of calcium carbonate whisker with a special focus on construction materials", *Constr. Build. Mater.*, **236**, 117613. https://doi.org/10.1016/j.conbuildmat.2019.117613.

Song, J.Y., Sim, Y., Jang, J., Hong, W.T. and Yun, T.S. (2020), "Near-surface soil stabilization by enzyme-induced carbonate precipitation for fugitive dust suppression", *Acta Geotechnica*, **15**(7), 1967-1980. https://doi.org/10.1007/s11440-019-00881-z.

Tao, H., He, Y. and Zhao, X. (2015), "Preparation and characterization of calcium carbonate–titanium dioxide core–shell ($CaCO_3$@ TiO_2) nanoparticles and application in the papermaking industry", *Powder Technol.*, **283**, 308-314. https://doi.org/10.1016/j.powtec.2015.05.039.

Trushina, D.B., Bukreeva, T.V. and Antipina, M.N. (2016), "Size-controlled synthesis of vaterite calcium carbonate by the mixing method: aiming for nanosized particles", *Crystal Growth Design*, **16**(3), 1311-1319. https://doi.org/10.1021/acs.cgd.5b01422.

Van Paassen, L.A., Harkes, M.P., Van Zwieten, G.A., Van der Zon, W.H., Van der Star, W.R.L. and Van Loosdrecht, M.C.M. (2009), "Scale up of BioGrout: a biological ground reinforcement method", *Proceedings of the 17th International Conference on Soil Mechanics and Geotechnical Engineering*, **1-4**, 2328-2333. https://doi.org/10.3233/978-1-60750-031-5-2328.

Wang, A., Li, J., Dong, Q., Wang, S., Jian, H., Wang, M. and Bai, S. (2019), "Preparation of microgels with ultrahigh payload of various hydrophilic and hydrophobic inorganic nanoparticle composites up to 92 wt%", *ACS Appl. Mater. Interfaces*, **11**(4), 4408-4415. https://doi.org/10.1021/acsami.8b20089.

Wang, J., Kong, Y., Liu, F., Shou, D., Tao, Y. and Qin, Y. (2018), "Construction of pH-responsive drug delivery platform with calcium carbonate microspheres induced by chitosan gels", *Ceramics Int.*, **44**(7), 7902-7907. https://doi.org/10.1016/j.ceramint.2018.01.227.

Wen, K., Bu, C., Liu, S., Li, Y. and Li, L. (2018), "Experimental investigation of flexure resistance performance of bio-beams reinforced with discrete randomly distributed fiber and bamboo", *Constr. Build. Mater.*, **176**, 241-249. https://doi.org/10.1016/j.conbuildmat.2018.05.032.

Wen, K., Li, Y., Amini, F. and Li, L. (2020), "Impact of bacteria and urease concentration on precipitation kinetics and crystal morphology of calcium carbonate", *Acta Geotechnica*, **15**(1), 17-27. https://doi.org/10.1007/s11440-019-00899-3.

Wu, C., Chu, J., Wu, S., Cheng, L. and van Paassen, L.A. (2019), "Microbially induced calcite precipitation along a circular flow channel under a constant flow condition", *Acta Geotechnica*, **14**(3), 673-683.https://doi.org/10.1007/s11440-018-0747-1.

Wu, L., Miao, L., Sun, X., Chen, R. and Wang, C. (2020), "Experimental study on solidifying sand using plant-derived urease induced calcium carbonate precipitation", *Chinese J. Geotech. Eng.*, **42**(4), 714-720. https://doi.org/10.11779/CJGE202004014.

Xiao, Y., Stuedlein, A.W., Ran, J., Evans, T.M., Cheng, L., Liu, H. and Chu, J. (2019), "Effect of particle shape on strength and stiffness of biocemented glass beads", *J. Geotech. Geoenviron. Eng.*, **145**(11), 06019016.https://doi.org/10.1061/(ASCE)GT.19435606.0002165.

Xiao, Y., Stuedlein, A.W., Pan, Z., Liu, H., Matthew Evans, T., He, X. and Van Paassen, L. A. (2020), "Toe-bearing capacity of precast concrete piles through biogrouting improvement", *J. Geotech. Geoenviron. Eng*., **146**(12). https://doi.org/10.1061/(ASCE)GT.1943-5606.0002404.

Xiao, Y., Stuedlein, A.W., He, X., Han, F., Evans, T.M., Pan, Z. and Van Paassen, L. (2021), "Lateral responses of a model pile in biocemented sand", *Int. J. Geomech.*, **21**(11), 06021027. https://doi.org/10.1061/(ASCE)GM.1943-5622.0002179.

Xu, J., Zhang, T., Jiang, Y., Yang, D., Qiu, F., Chen, Q. and Yu, Z. (2020), "Preparation of self-healing acrylic copolymer composite coatings for application in protection of paper cultural relics", *Polymer Eng. Sci.*, **60**(2), 288-296. https://doi.org/10.1002/pen.25282.

Xu, X., Guo, H., Li, M. and Deng, X. (2021), "Bio-cementation improvement via $CaCO_3$ cementation pattern and crystal polymorph: A review", *Constr. Buildi. Mater.*, **297**, 123478. https://doi.org/10.1016/J.CONBUILDMAT.2021.123478.

Yang, J. and Shih, S.(2010), "Preparation of high school $CaCO_3$ for SO_2 removal by absorption of CO_2 in aqueous suspensions of $Ca(OH)_2$", *Powder Technol.*, **202**, 101-110.

Yang, Y., Li, M., Tao, X., Zhang, S., He, J., Zhu, L. and Wen, K. (2022), "The effect of nucleating agents on enzyme-induced carbonate precipitation and corresponding microscopic mechanisms", *Materials*, **15**(17), 5814. https://doi.org/10.3390/MA15175814.

Yuan, H., Ren, G., Liu, K., Zheng, W. and Zhao, Z. (2020), "Experimental study of EICP combined with organic materials for silt improvement in the yellow river flood area", *Appl. Sci.*, **10**(21), 7678. https://doi.org/10.3390/APP10217678.

Zhao, L., Zhang, Y., Miao, Y. and Nie, L. (2016), "Controlled synthesis, characterization and application of hydrophobic calcium carbonate nanoparticles in PVC", *Powder Technol.*, **288**, 184-190. https://doi.org/10.1016/j.powtec.2015.11.001.

Zhao, X., Feng, Q., Li, J. and Peng J. (2019), "Research of influences of temperature on amount of microbially induced carbonate precipitation", *Ind. Constr.*, **49**(11), 88-92+112. https://doi.org/10.13204/j.gyjz201911015

Zhao, Q., Li, L., Li, C., Li, M., Amini, F. and Zhang, H. (2014), "Factors affecting improvement of engineering properties of MICP-treated soil catalyzed by bacteria and urease", *J. Mater. Civil Eng.*, **26**(12), 04014094. https://doi.org/10.1061/(ASCE)MT.1943-5533.0001013.

Zhuravlev, Y.N. and Atuchin, V.V. (2020), "Comprehensive density functional theory studies of vibrational spectra of carbonates", *Nanomater.*, **10**(11), 2275. https://doi.org/10.3390/nano10112275.

CC